Safety Implications of Cr-Coated ATF Cladding: Realizable Benefits and Inherent Limitations

SungHoon Joung[a], Youho Lee[a*]
[a] *Department of Nuclear Engineering, Seoul National University, Gwanak-ro 1, Gwanak-gu, Seoul 08826, Republic of Korea*

Keywords : Cr-coated ATF, Post quench ductility, ECCS criteria, Zr-Cr eutectic, Secondary hydriding

1. Introduction

Cr-coated Accident Tolerant Fuel (ATF) cladding is considered as one of the most promising concepts for commercialization due to its superior high-temperature steam oxidation resistance while maintaining the mechanical characteristics of conventional zirconium alloys [1-3]. Under the current regulatory framework (10 CFR 50.46), mechanical integrity of cladding is evaluated primarily based on Peak Cladding Temperature (1204 ℃) and Equivalent Cladding Reacted (17%) limits, which were established on the basis of oxidation-induced embrittlement of zirconium alloy cladding [4]. However, the introduction of chromium coating raises important questions regarding the applicability of the existing ECR and PCT criteria. Although the chromium coating effectively suppresses outer-wall steam oxidation and delays oxidation kinetics, the substrate matrix of Cr-coated ATF remains a zirconium alloy. In addition, the formation of a Zr–Cr eutectic phase at approximately 1320 ℃, which does not occur in conventional zirconium alloy cladding, introduces a new phenomenon that must be examined with respect to structural integrity and post-quench ductility [5-7]. Furthermore, under integral Loss Of Coolant Accident conditions involving ballooning and burst, burst-induced inner-wall oxidation promotes hydrogen uptake, resulting in secondary hydriding. This mechanism is not unique to Cr-coated ATF but inherent to zirconium-based cladding [8-11]. Nevertheless, the current oxidation-based regulatory criteria do not explicitly account for the embrittlement associated with secondary hydride formation following burst. Accordingly, a comprehensive evaluation of the regulatory applicability of the current ECR and PCT limits to Cr-coated zirconium alloy cladding remains necessary. In this study, the applicability of the current ECR and PCT limits to Cr-coated ATF cladding was experimentally evaluated under integral LOCA conditions. In addition, the impact of burst-induced secondary hydriding on residual ductility was systematically assessed.

2. Methods and Results

In this study, a series of experiments were conducted to assess the Equivalent Cladding Reacted (ECR) and Peak Cladding Temperature (PCT) limits of Cr-coated accident tolerant fuel (ATF) cladding under LOCA conditions. In addition, secondary hydriding was examined to determine its influence on post-quench ductility, particularly in burst scenarios where hydrogen uptake may alter cladding behavior independently of oxidation-based limits.

2.1 Experimental setup

Figure 1 illustrates the experimental facilities employed in this study. The integral LOCA facility(*i*-LOCA) was used to simulate the integral thermo-mechanical behavior of 1.5-meter-long cladding under LOCA conditions, including ballooning, burst, high-temperature steam oxidation, and subsequent quenching [12, 13]. Induction heating was applied to achieve rapid temperature rise up to 1500 ℃, ensuring representative burst behavior. The high-temperature oxidation facility was utilized to expose cladding specimens to controlled steam or oxygen-free environments, enabling the analysis of oxidation behavior and eutectic formation under well-defined thermal conditions. The performance and reliability of both facilities have been validated in previous studies [14-16].

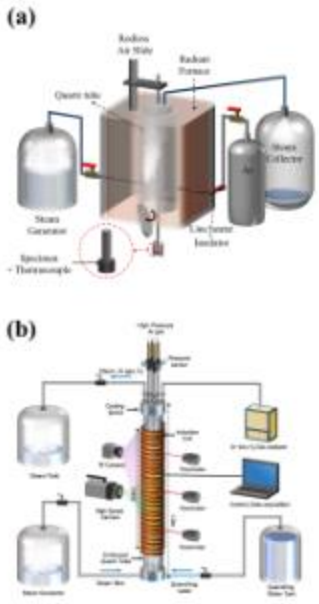

Fig. 1. Schematics of (a) high-temperature oxidation facility and (b) integral LOCA facility [17].

After exposure at high-temperature steam an oxygen-free environment, residual ductility was evaluated using the ring compression test (RCT) with a universal testing machine (INSTRON-8516). A schematic of the RCT setup is presented in **Fig. 2(a)**. To minimize azimuthal temperature gradients, aluminum insulators were installed on the upper and lower compression jigs. The test was initiated when the specimen temperature at four azimuthal positions (top, bottom, left, and right) reached 135 ± 3 ℃, and compression rate was set at 0.033 mm/s, following the experimental protocol of the U.S. NRC [18]. A representative load–displacement curve obtained from the RCT is shown in **Fig. 2(b)**. The load drop point was defined as the location where the load sudden decreased by more than 30%, indicating through-wall crack propagation. The offset strain was then calculated by extending the pseudo-stiffness line through the load drop point and determining its intersection with the displacement axis, following the experimental protocol of the U.S. NRC [18].

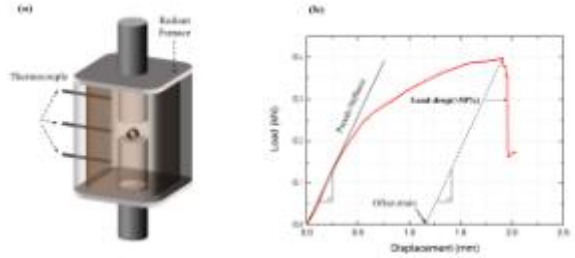

Fig. 2. (a) Schematic diagram of the ring compression test (RCT) facility and (b) representative load–displacement curve with parameters obtained from the RCT [17].

Additionally, Cross-sectional microstructures of the specimens were analyzed using scanning electron microscopy (SEM). Oxygen concentration profiles across the oxide, α(O), and β-layer regions were measured by electron probe microanalysis (EPMA). The hydrogen content of the specimens after integral LOCA testing was quantified using an oxygen–nitrogen–hydrogen (ONH) analyzer to assess hydrogen uptake.

2.2 Assessment of the ECR limit for Cr-coated ATF

Figure 3 shows the WG-ECR to offset strain curves for bare Zr-1.1Nb and Cr-coated Zr-1.1Nb, with the ductile-to-brittle transition line proposed by the U.S. NRC [19]. At the same WG-ECR, the Cr-coated specimens has lower offset strain compared to the bare specimens. As a result, Cr-coated Zr-1.1Nb reaches the ductile-to-brittle transition at a lower WG-ECR compared to the bare cladding. The ECR limit for Cr-coated Zr-1.1Nb obtained in this study was 19%, which is lower than that of the bare cladding with the same substrate.

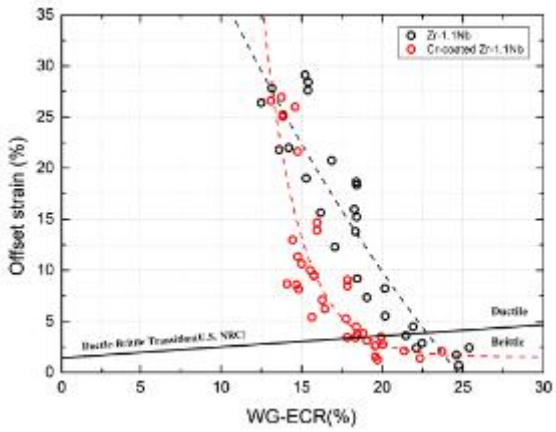

Fig. 3. WG-ECR to offset strain curve for bare and Cr-coated Zr-1.1Nb with the ductile to brittle criteria from U.S. NRC [19].

The reduction in the ECR limit for Cr-coated ATF can be explained by the crack initiation and propagation behavior shown in **Fig. A** in Appendix. In the Cr-coated specimens, cracks were initiated from the $ZrCr_2$ layer formed at the Zr/Cr interface. This layer was adjacent to the oxygen-enriched α(O) region, which thickened due to oxygen diffusion through the Cr coating during high-temperature steam oxidation. The increased oxygen concentration in the interfacial Zr matrix promoted crack initiation under tensile stress during the Ring Compression Test (RCT). Subsequently, the initiated cracks propagated into the Zr matrix as through-wall cracks, thereby accelerating the ductile-to-brittle transition. In other words, premature crack initiation at the $ZrCr_2$ interface was primarily responsible for the reduced ECR limit observed in the Cr-coated Zr-1.1Nb. In addition, thermal expansion mismatch among the Zr substrate, Cr coating, and the interfacial $ZrCr_2$ layer may also influence crack initiation behavior during quenching. Because these phases possess different coefficients of thermal expansion, rapid cooling from high-temperature oxidation can introduce additional interfacial stress due to differential thermal contraction. Such thermally induced stresses may further facilitate crack nucleation within the brittle intermetallic layer. However, the present study did not quantitatively evaluate residual stress, and thus the extent of its contribution remains to be investigated. However, this comparison reflects the mechanical behavior at an equivalent WG-ECR and does not account for differences in oxidation kinetics under accident conditions. Since the Cr coating effectively suppresses outer-wall oxidation, oxidation of Cr-coated ATF proceeds predominantly from the inner surface. As a result, the time required to reach the same ECR level is longer than that of bare cladding. Therefore, from the perspective of oxidation delay and accident coping time, Cr-coated ATF provides a clear advantage [16, 20].

Nevertheless, whether the approximately 19% of ECR limit for Cr-coated ATF derived in this study

justifies an upward revision of the current 17% regulatory limit warrants careful consideration. Although modern zirconium alloys have demonstrated ductile-to-brittle transition limits exceeding 17% [21, 22], regulatory criteria have historically been established based on conservatism and simplicity, adopting the most conservative value and applying it uniformly across cladding materials. In this context, an increase of approximately 2 percentage points in the ECR limit for Cr-coated ATF may not translate into a meaningful enhancement of regulatory safety. Rather than introducing a design-specific criterion, maintaining the existing 17% limit may therefore represent a more rational and consistent approach. The primary benefit of the Cr coating lies not in increasing the allowable ECR limit itself, but in extending the time required to reach the regulatory limit (i.e., accident coping time) through delayed oxidation.

2.3 Assessment of the PCT limit for Cr-coated ATF

Previous study have reported that the Zr–Cr eutectic reaction does not directly lead to structural collapse of the cladding [23]. Consistent with these findings, the results of the *i*-LOCA test conducted in this study showed that, despite the occurrence of the eutectic reaction, no structural failure such as melting was observed. Therefore, the Zr-Cr eutectic reaction should not be interpreted as equivalent to a melting phenomenon, but rather understood as a potential embrittlement mechanism that may influence the mechanical integrity of the cladding.

Figure 4(a) shows the offset strain based on the oxidation time for bare and Cr-coated Zr-1.1Nb oxidized above the eutectic onset temperature (~1320 ℃). Cross-sectional SEM images for Cr-coated specimens confirmed the formation of a Zr–Cr eutectic layer in the Cr-coated specimens. However, despite the occurrence of the eutectic reaction, the ductility of the Cr-coated specimens was comparable to that of the bare Zr-1.1Nb. These results indicate that, although the Zr–Cr eutectic reaction may contribute to ductility reduction, its impact on the ductility is not dominant. Considering that no structural collapse was observed despite the occurrence of the eutectic reaction, the Zr–Cr eutectic should not be regarded as an independent melting threat. Rather, it is more appropriately interpreted as embrittlement mechanism.

However, a more pronounced difference is observed when comparing specimens oxidized at different temperatures, as shown in **Fig. 4(b)**. When the WG-ECR to offset strain behavior of Zr-1.1Nb oxidized at 1204 ℃ (current PCT limit) and 1332 ℃ (above the eutectic onset temperature) is compared, the specimen oxidized at 1332 ℃ exhibits significantly lower ductility even at the same WG-ECR value. For example, at approximately 13% WG-ECR, the specimen oxidized at 1204 ℃ retains a substantial ductility, whereas the specimen oxidized at 1332 ℃ shows an offset strain close to zero. This indicates that ductility degradation is not solely determined by the absolute ECR value, but is strongly influenced by differences in oxygen diffusion behavior associated with oxidation temperature.

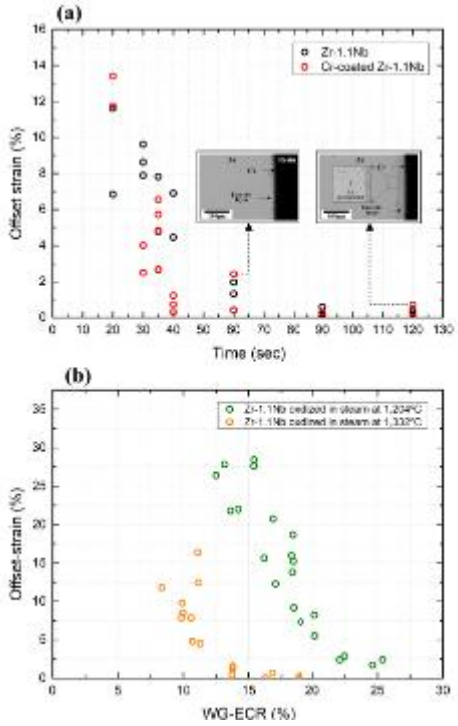

Fig. 4. (a) Time to offset strain curves for bare and Cr-coated Zr-1.1Nb with cross-sectional SEM images after oxidation above eutectic temperature; (b) WG-ECR to offset strain curves for Zr-1.1Nb oxidized at 1204 ℃ and 1332 ℃.

In this regard, **Fig. B** in Appendix compares the oxygen concentration within the β-layer at the same WG-ECR under the two oxidation temperature conditions. The specimen oxidized at 1332 ℃ exhibits a markedly higher average oxygen concentration in the β-layer compared to that oxidized at 1204 ℃. At elevated temperatures, the oxygen diffusion coefficient increases significantly, allowing oxygen to penetrate more rapidly into the Zr matrix. As a result, the oxygen concentration within the β-layer increases, leading to enhanced solid-solution hardening[24]. Consequently, ductility is degraded much more rapidly even at the same ECR value.

In summary, the critical issue in Cr-coated ATF is not the Zr–Cr eutectic reaction itself, but the oxidation behavior in the temperature where the eutectic reaction occurs. In this temperature range, oxygen-induced embrittlement of the zirconium alloy matrix is dominant. This behavior is intrinsically governed by the fact that the substrate material remains a zirconium alloy, regardless of the presence of the Cr coating. Indeed, excessive oxygen dissolution and the resulting rapid embrittlement at elevated temperatures were already key considerations in establishing the 1204 ℃ PCT limit in the 1970s [24-27]. Accordingly, the results

obtained in this study indicate that the presence of the Zr–Cr eutectic reaction alone does not constitute a sufficient basis for modifying the existing PCT limit. Rather, maintaining the current 1204 ℃ PCT limit for Cr-coated ATF ensures the nuclear safety and mechanical integrity of Cr-coated ATF.

2.4 Impact of secondary hydriding on ductility

Under the current LOCA regulatory framework, residual ductility is primarily evaluated based on the extent of oxidation, typically quantified by the Equivalent Cladding Reacted (ECR), and the Peak Cladding Temperature (PCT). This approach is founded on the assumption that the cladding must retain sufficient ductility after high-temperature oxidation followed by quenching [4, 18, 28]. However, in order for meaningful oxidation to occur under LOCA conditions, ballooning and burst commonly precede or accompany the oxidation process. In this sense, an ECR-based evaluation inherently presupposes the possibility of burst. Once burst occurs, high-temperature steam directly enters the inner surface of the cladding through the burst opening, leading to rapid inner-wall oxidation. During this process, hydrogen generated during oxidation diffuses into the high-temperature Zr matrix and is absorbed [29-31]. Upon subsequent cooling, the dissolved hydrogen precipitates as hydrides. This secondary hydriding mechanism is fundamentally different from oxidation-induced embrittlement and can significantly degrade ductility. Importantly, its impact is not directly proportional to the ECR value.

Figure 5 shows the axial distribution of hydrogen concentration in bare and Cr-coated Zr-1.1Nb claddings following the i-LOCA test (1200 ± 25 ℃, 5 min oxidation). In both specimens, the hydrogen concentration exceeded 2000 wppm in the vicinity of the burst opening, exhibiting a similar M-shaped distribution along the axial direction. Notably, Cr-coated ATF claddings exhibited hydrogen pickup behavior comparable to that of bare zirconium-based alloy claddings. These results indicate that, although the Cr coating effectively suppresses outer-surface oxidation, it does not mitigate hydrogen ingress associated with inner-wall oxidation following burst. Since secondary hydriding is primarily driven by steam oxidation at the inner surface near the burst opening, the protective benefit of the Cr coating against steam oxidation becomes largely diminished under burst conditions. Consequently, under secondary hydriding conditions, the oxidation-resistance advantage of Cr-coated ATF is substantially offset.

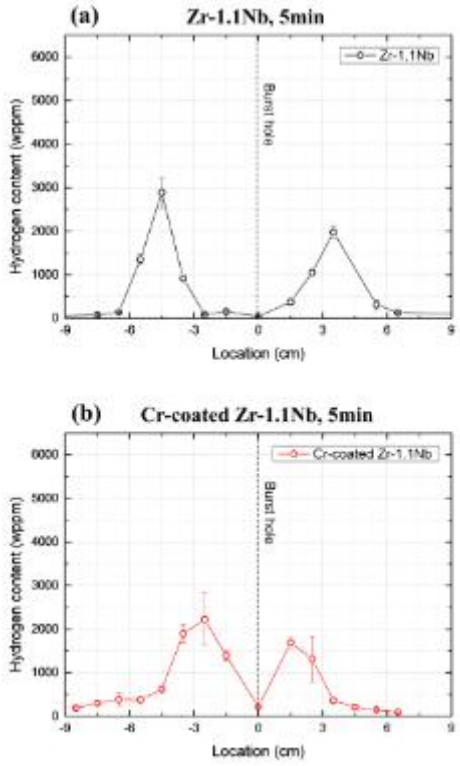

Fig. 5. Axial distributions of hydrogen content in bare and Cr-coated Zr-1.1Nb following i-LOCA test (oxidized at 1200 ± 25 ℃ for 5 min)

Figure 6 compares the WG-ECR–offset strain behavior under identical oxidation conditions with the conventional PQD test results. In the PQD tests [22], ductility progressively decreases with increasing ECR, reflecting the typical oxidation-induced embrittlement associated with the growth of the ZrO_2 layer and the oxygen-enriched α(O) phase. In contrast, the i-LOCA specimens exhibit a much more pronounced loss of ductility. Even at approximately 10–12% WG-ECR, the offset strain drops sharply to below 5%. This behavior stands in clear contrast to the PQD specimens, which retain more than 25% offset strain at comparable ECR levels. These results indicate that the degradation of ductility in the i-LOCA specimens cannot be explained by oxygen-induced embrittlement alone.

This pronounced difference is attributed to the effect of secondary hydriding. Even at the same WG-ECR, once the hydrogen concentration increases to approximately 1000–2000 wppm or higher, hydrogen-induced embrittlement becomes dominant over oxidation-induced embrittlement, leading to a rapid loss of ductility. In some specimens, the hydrogen concentration exceeded 6000 wppm, resulting in such severe brittleness that RCT specimens could not be prepared. Importantly, this behavior was observed in both bare Zr-1.1Nb and Cr-coated Zr-1.1Nb, indicating that the presence of the Cr coating does not mitigate embrittlement due to secondary hydriding once burst-induced inner-wall oxidation occurs. These results

demonstrate that, under LOCA conditions involving burst, ductility degradation is governed primarily by hydrogen accumulation rather than oxidation alone.

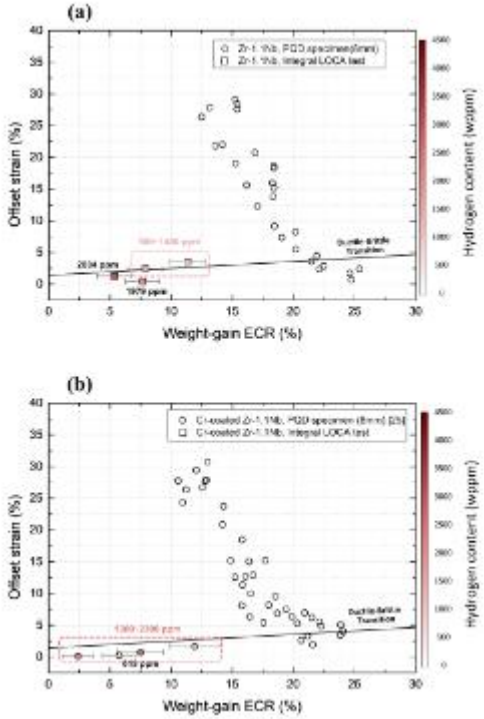

Fig. 6. WG-ECR to offset strain curves for bare and Cr-coated Zr-1.1Nb oxidized at 1200 ± 25 ℃ for 5 min, compared with previous PQD test results [22].

However, secondary hydriding is not explicitly addressed within the current ECCS criteria, which primarily focus on oxidation and hydrogen absorbed during pre-transient oxidation. As shown in this study, secondary hydriding can dominate ductility degradation even at relatively low ECR. Therefore, the safety implications of Cr-coated ATF cannot be assessed solely on the basis of oxidation resistance. While the Cr coating effectively suppresses outer-wall oxidation, its structural advantage is significantly reduced once ballooning and burst occur.

3. Conclusions

In this study, the ECR and PCT limits for Cr-coated ATF, as well as the impact of burst-induced secondary hydriding on residual ductility, were experimentally evaluated. The results demonstrated that the Cr coating significantly delayed high-temperature steam oxidation. Although the Zr–Cr eutectic reaction occurred, it did not lead to macroscopic melting or structural collapse of the cladding. These findings indicate that the current ECR and PCT criteria is applicable for Cr-coated ATF. However, once burst occurred, rapid inner-wall oxidation resulted in substantial hydrogen uptake, leading to pronounced secondary hydriding. This hydrogen-induced embrittlement caused a dramatic loss of ductility even at relatively low ECR. These results indicate that structural integrity under LOCA conditions cannot be explained solely by oxidation behavior, as post-burst hydrogen accumulation may play a dominant role in governing ductile-to-brittle transition.

Taken together, the present findings demonstrate that while Cr coating provides a clear oxidation-resistance benefit, its structural advantage can be conditionally limited by burst-induced secondary hydriding. Conversely, under operating and design conditions where burst is effectively suppressed, the oxidation-resistance advantage of Cr coating can be more fully retained. Ultimately, the practical benefit of Cr-coated ATF is not automatically realized by material improvement alone; rather, it depends on the alignment of material performance with operating conditions and regulatory interpretation.

4. APPENDIX

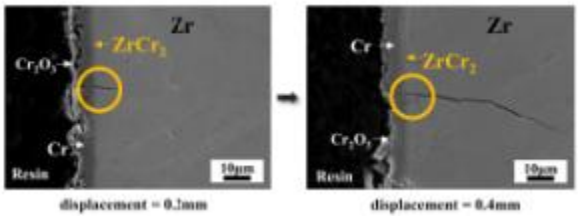

Fig. A. Crack initiation and propagation of the Cr-coated Zr-1.1Nb.

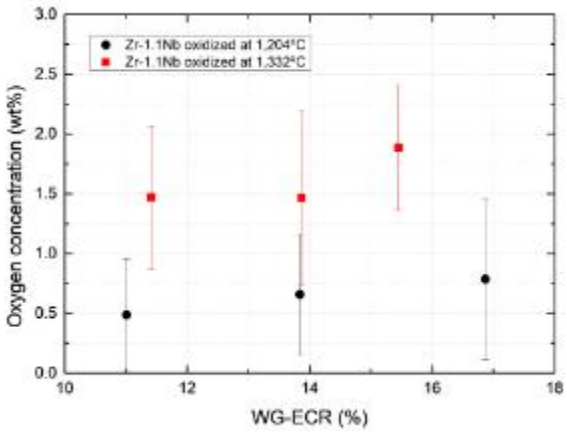

Fig. B. Oxygen concentration in the β-layer for Zr-1.1Nb oxidized at 1204 ℃ and 1332 ℃ based on WG-ECR.

Acknowledgement

This work was supported by the Korea Institute of Energy Technology Evaluation and Planning(KETEP) and the Ministry of Climate, Energy & Environment(MCEE) of the Republic of Korea (No. RS-2025-02633904, Center for Advanced Nuclear Fuel Innovation).

REFERENCES

[1] H.-G. Kim, I.-H. Kim, Y.-I. Jung, D.-J. Park, J.-H. Yang, Y.-H. Koo, Development of surface modified Zr cladding by coating technology for ATF, Proceedings of the Top Fuel (2016) 1157-1163.
[2] A. Michau, F. Maury, F. Schuster, F. Lomello, J.C. Brachet, E. Rouesne, M. Le Saux, R. Boichot, M. Pons, High-temperature oxidation resistance of chromium-based coatings deposited by DLI-MOCVD for enhanced protection of the inner surface of long tubes, Surf Coat Tech 349 (2018) 1048-1057.
[3] K.A. Terrani, Accident tolerant fuel cladding development: Promise, status, and challenges, Journal of Nuclear Materials 501 (2018) 13-30.
[4] "Acceptance criteria for emergency core cooling systems for light water cooled nuclear power reactors," and Appendix K to 10 CFR 50. "ECCS Evaluation Models, U.S. Federal Register 39 (3), 10 CFR 50.46.
[5] J.C. Brachet, E. Rouesne, J. Ribis, T. Guilbert, S. Urvoy, G. Nony, C. Toffolon-Masclet, M. Le Saux, N. Chaabane, H. Palancher, A. David, J. Bischoff, J. Augereau, E. Pouillier, High temperature steam oxidation of chromium-coated zirconium-based alloys: Kinetics and process, Corrosion Science 167 (2020).
[6] D. Kim, M. Ševeček, Y. Lee, Characterization of eutectic reaction of Cr and Cr/CrN coated zircaloy accident tolerant fuel cladding, Nuclear Engineering and Technology (2023).
[7] D. Kim, M. Steinbrück, M. Grosse, C. Tang, Y. Lee, Eutectic reaction and oxidation behavior of Cr-coated Zircaloy-4 accident-tolerant fuel cladding under various heating rates, Journal of Nuclear Materials 583 (2023) 154538.
[8] T. Furuta, S. Kawasaki, M. Hashimoto, T. Otomo, Zircaloy-clad fuel rod burst behavior under simulated loss-of-coolant condition in pressurized water reactors, Journal of nuclear Science and Technology 15(10) (1978) 736-744.
[9] T. Furuta, H. Uetsuka, S. Kawasaki, Ductility loss of zircaloy cladding by inner-surface oxidation during high temperature transient, Journal of Nuclear Science and Technology 18(10) (1981) 802-810.
[10] S. Kawasaki, T. Furuta, M. Suzuki, Oxidation of Zircaloy-4 under high temperature steam atmosphere and its effect on ductility of cladding, Journal of nuclear science and technology 15(8) (1978) 589-596.
[11] H. Uetsuka, T. Furuta, S. Kawasaki, Zircaloy-4 cladding embrittlement due to inner surface oxidation under simulated loss-of-coolant condition, Journal of Nuclear Science and Technology 18(9) (1981) 705-717.
[12] H. Yook, S. Joung, C. Lee, Y. Lee, Integral LOCA experiments to study FFRD behavior of high burnup nuclear fuels, Nuclear Engineering and Design 429 (2024) 113633.
[13] H. Yook, S. Joung, Y. Lee, Ballooning, Burst and Oxidation behavior of Cr-coated ATF cladding during LOCA Transactions of the Korean Nuclear Society Spring Meeting Korean Nuclear Society, Jeju, Korea, 2024.
[14] K. Keum, Y. Lee, Effect of cooling rate on the residual ductility of Post-LOCA Zircaloy-4 cladding, Journal of Nuclear Materials 541 (2020) 152405.
[15] H. Yook, Y. Lee, Post-LOCA ductility assessment of Zr-Nb Alloy from 1100 degrees C to 1300 degrees C to explore variable peak cladding temperature and equivalent cladding reacted safety criteria, Journal of Nuclear Materials 567 (2022).
[16] H. Yook, K. Shirvan, B. Phillips, Y. Lee, Post-LOCA ductility of Cr-coated cladding and its embrittlement limit, Journal of Nuclear Materials 558 (2022).
[17] S. Joung, D. Woo, Y. Lee, Missing Half the Story: Impact of Secondary Hydriding on Post-Loca Ductility of Cr-Coated Zirconium Alloy Accident Tolerant Fuel Cladding, Available at SSRN 5290915.
[18] USNRC. Regulatory Guide 1.223-Determing post quench ductility, Washington. D.C., USA, 2018.
[19] U.S.N.R.C.U.S. NRC), ESTABLISHING ANALYTICAL LIMITS FOR ZIRCONIUM-ALLOY CLADDING MATERIAL, REGULATORY GUIDE, U.S. NUCLEAR REGULATORY COMMISSION (U.S. NRC), 2014.
[20] A. Gurgen, K. Shirvan, Estimation of coping time in pressurized water reactors for near term accident tolerant fuel claddings, Nuclear Engineering and Design 337 (2018) 38-50.
[21] M. Billone, T. Burtseva, Y. Yan, Ductile-to-Brittle Transition Temperature for High Burnup Zircaloy-4 and ZIRLO (TM) Cladding Alloys Exposed to Simulated Drying Storage Conditions, Argonne National Lab.(ANL), Argonne, IL (United States), 2013.
[22] S. Joung, J. Kim, M. Ševeček, J. Stuckert, Y. Lee, Post-quench ductility limits of coated ATF with various zirconium-based alloys and coating designs, Journal of Nuclear Materials 591 (2024) 154915.
[23] B. Kweon, H. Yook, Y. Lee, Experimental Investigation of Eutectic Formation in Cr coated Accident Tolerant Fuel Cladding and its Safety Implications, Transactions of the Korean Nuclear Society Spring Meeting Korean Nuclear Society, Jeju, Korea, 2024
[24] H.M. Chung, Fuel behavior under loss-of-coolant accident situations, Nuclear engineering and technology 37(4) (2005) 327-362.
[25] D. Hobson, Ductile-brittle behavior of Zircaloy fuel cladding, Oak Ridge National Lab.(ORNL), Oak Ridge, TN (United States), 1972.
[26] D. Hobson, P. Rittenhouse, EMBRITTLEMENT OF ZIRCALOY-CLAD FUEL RODS BY STEAM DURING LOCA TRANSIENTS, Oak Ridge National Lab.(ORNL), Oak Ridge, TN (United States), 1972.
[27] A.E. Commission, Supplemental Testimony of the Regulatory Staff Docket RM-50-1, Atomic Energy Commission Atomic Energy Commission 1972.
[28] NUREG/CP-6967-Cladding Embrittlement During Postulated Loss-of-Coolant Accidents U.S.NRC, 2008.
[29] I. Alakiozidis, M.L.N. de Sousa, A. Gauthier, C. Hunt, M. Maric, A. Ambard, Z. Shah, P. Frankel, Semi-integral LOCA testing of Cr-coated Optimized ZIRLOTM claddings, Journal of Nuclear Materials 610 (2025) 155766.
[30] J.-C. Brachet, D. Hamon, M. Le Saux, V. Vandenberghe, C. Toffolon-Masclet, E. Rouesne, S. Urvoy, J.-L. Béchade, C. Raepsaet, J.-L. Lacour, “Study of secondary hydriding at high temperature in zirconium based nuclear fuel cladding tubes by coupling information from neutron radiography/tomography, electron probe micro analysis, micro elastic recoil detection analysis and laser induced breakdown spectroscopy microprobe, Journal of Nuclear Materials 488 (2017) 267-286.
[31] M. Grosse, C. Roessger, J. Stuckert, M. Steinbrueck, A. Kaestner, N. Kardjilov, B. Schillinger, Neutron imaging investigations of the secondary hydriding of nuclear fuel cladding alloys during loss of coolant accidents, Physics Procedia 69 (2015) 436-444.